Requirements for a GaAsBi 1 eV sub-cell in a GaAs based multi-junction solar cell

T Thomas[1], A Mellor[1], N P Hylton[1], M Führer[1], D Alonso-Álvarez[1], A Braun[1], N J Ekins-Daukes[1], J P R David[2], S J Sweeney[3]

1. Imperial College London, London, U.K., 2. University of Sheffield, Sheffield, U.K., 3. Advanced Technology Institute and Department of Physics, University of Surrey, Guildford, Surrey, U.K.

E-mail: tomos.thomas08@imperial.ac.uk

Abstract. Multi-junction solar cells achieve high efficiency by stacking sub-cells of different bandgaps (typically GaInP/GaAs/Ge) resulting in efficiencies in excess of 40%. The efficiency can be improved by introducing a 1 eV absorber into the stack, either replacing Ge in a triple-junction configuration or on top of Ge in a quad-junction configuration. $GaAs_{0.94}Bi_{0.06}$ yields a direct-gap at 1 eV with only 0.7% strain on GaAs and the feasibility of the material has been demonstrated from GaAsBi photodetector devices. The relatively high absorption coefficient of GaAsBi suggests sufficient current can be generated to match the sub-cell photocurrent from the other sub-cells of a standard multi-junction solar cell. However, minority carrier transport and background doping levels place constraints on both *p/n* and *p-i-n* diode configurations. In the possible case of short minority carrier diffusion lengths we recommend the use of a *p-i-n* diode, and predict the material parameters that are necessary to achieve high efficiencies in a GaInP/GaAs/GaAsBi/Ge quad-junction cell.

1. Introduction

Multi-junction solar cells are the highest performing class of solar cells in terms of efficiency. They are composed of semiconductor diodes of multiple bandgaps, connected in series, and achieve a fundamental efficiency advantage over single bandgap cells. However, the series connection enforces a narrow range of bandgap energies, since each sub-cell should photogenerate equal currents and must therefore be carefully matched to the solar spectrum. Common commercial triple-junction cells are based on a lattice-matched combination of GaInP/GaAs/Ge with bandgaps of 1.9/1.42/0.66 eV on Ge substrate. However, a 1 eV sub-cell can provide higher efficiency than 0.66 eV Ge. Commercially, triple junction solar cells are available with efficiencies in excess of 40% and research is now proceeding towards quad-junction and five-junction structures, creating new records for efficiency under concentration [1] and at one sun [2]. Two different approaches to these structures have been utilized in these recent results in order to create a 1 eV sub-cell: wafer-bonding [1, 2] and inverted metamorphic (IMM) growth techniques [3, 4]. These allow engineering of sub-cell bandgaps to those desirable for the solar spectrum, but come with some disadvantages such as the need for two substrates, or

the unavoidable introduction of dislocations, which can increase production costs or decrease material quality respectively. The 1 eV bandgap has been successfully implemented in a lattice-matched record triple junction cell using dilute nitride GaInAsNSb material lattice-matched to GaAs [5]. With N affecting the conduction band and Bi mainly affecting the valence band of their respective alloys, there is therefore great interest in dilute bismide alloys such as 1 eV GaAsBiN lattice-matched to GaAs or Ge [6] [7]. In this study, we restrict ourselves to the investigation of $GaAs_{0.94}Bi_{0.06}$ (referred to simply as GaAsBi in the rest of this work) that yields a direct-gap at 1 eV with only 0.7% strain on GaAs [8]. This is significantly less strain than the 1.9% created by growing 1 eV $In_{0.27}Ga_{0.73}As$ on GaAs, as is done for IMM cell architectures [9]. $GaAs_{1-x}Bi_x$ was first demonstrated using metal-organic chemical vapour deposition [10] but bismuth incorporation as high as 22% has been demonstrated with molecular beam epitaxy [11]. The feasibility of 1 eV bulk GaAsBi devices has been demonstrated using photodetectors [12] and light-emitting diodes [13] and lasers [14] have been demonstrated at different bandgaps. In this work we calculate some of the requirements for the GaAsBi sub-cell in a 1.9/1.42/1.05/0.66 eV GaInP/GaAs/GaAsBi/Ge structure and project the efficiency under concentration. Realistic values for loss mechanisms are used to determine whether a GaAsBi-based quad-junction (4J) structure can provide performance comparable to the current state-of-the-art. A framework is used that relates GaAsBi sub-cell current to junction depletion width and minority carrier diffusion length and relates sub-cell voltage to junction depletion width and minority carrier lifetime. Current values for these parameters are discussed, as well as challenges with using GaAsBi.

2. Simulation method

A solar cell can be simply represented by an equivalent circuit commonly known as the double diode model (shown in figure 1). In this model the photogenerated short-circuit current acts as a current source and there are two recombination diodes with different ideality factors, representing recombination in different sections of the device. This is summarized by equation (1). A multi-junction solar cell can be represented by connecting circuits in series, with a series resistance and parallel (shunt) resistance. This model, with equation (1) representing each sub-cell, is used to calculate the results in this report.

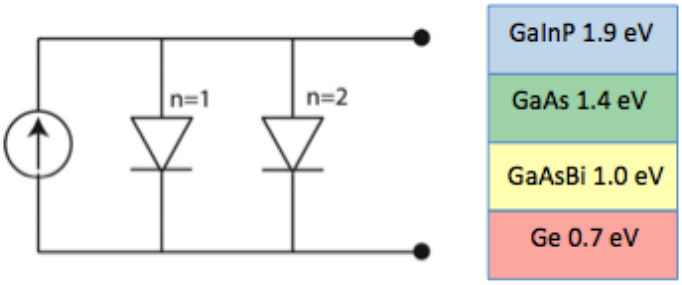

Figure 1. (left) Double diode model equivalent circuit for sub-cell. Series resistance not

shown. n=1 recombination is assumed to be radiative. n=2 recombination is assumed to be non-radiative (Shockley-Read-Hall (SRH) recombination). (right) Schematic of the quad-junction structure evaluated in this work.

$$\mathrm{I} = I_{SC} - I_{01}\left(e^{\frac{q(V+IR_S)}{k_BT}} - 1\right) - I_{02}\left(e^{\frac{q(V+IR_S)}{2k_BT}} - 1\right) \quad (1)$$

Equation (1) is the diode equation, where I is the current through the sub-cell, I_{SC} is the short-circuit current, I_{01} is recombination in the quasi-neutral regions (the non-depleted regions of the base and emitter), I_{02} is recombination in the depletion region, V is voltage, R_S is series resistance, T is temperature and k_B is Boltzmann's constant. For a solar cell operating under highly concentrated illumination, the recombination associated with I_{01} will often dominate. The recombination in each region is discussed further in section 1.2 below.

The extrinsic loss mechanisms considered in our model include series resistance, front contact grid metal coverage and reflection of photons. The series resistance and metal coverage are linked and must be optimised in concentrator cells – more metal lowers series resistance but obscures more of the surface of the cell. In this work a value of series resistance of 12.25 mΩcm^2 is used, allowing the cell efficiency to peak at 1000 times concentration. The approximate corresponding metal coverage gives a 5% reduction in light absorption due to grid shading. Reflection determined by the properties of the anti-reflection coating is discussed in the next section.

1.1. Short-circuit current

The short-circuit current for each sub-cell is initially calculated using the Beer-Lambert law from the absorption coefficient and thickness of the sub-cell in question along with a typical dual-layer anti-reflection coating profile used in a multi-junction solar cell. For the non-GaAsBi sub-cells, each photon absorbed is assumed to produce one electron-hole pair that is then collected, implying unity internal quantum efficiency. The absorption coefficients for different materials were either calculated with a critical point interpolation method [15] or taken from literature [12]. Along with that reported in [12], an absorption coefficient for GaAsBi was reported in [16] which produces very similar photocurrent to [12] using the Beer-Lambert method discussed above. The anti-reflection coating (dual layer Al_2O_3/TiO_2) Fresnel coefficients were calculated using a thin-film transfer matrix method assuming a GaAs substrate and air interface. As the lowest sub-cell current limits the total current through a multi-junction solar cell, high efficiency only results when the currents photogenerated in the sub-cells are similar. The thicknesses of each sub-cell are varied to balance the sub-cell currents and determine the thickness of GaAsBi required for the best performing cell. This leads to interdependency in cell design that in this study is determined by the GaAsBi absorption coefficient. First the optimal thickness for the GaAsBi sub-cell is calculated under the assumption of perfect photon collection, but this approximation is subsequently relaxed and the external

quantum efficiency is calculated as a function of material parameters using an analytical solution to the semiconductor drift-diffusion transport equations [17]. A low surface recombination velocity of 100 cm/s is assumed as a boundary condition. This allows us to establish target material parameters for the useful implementation of GaAsBi sub-cells in multi-junction devices – minority carrier diffusion length and junction depletion width in the case of short-circuit current.

1.2. Recombination mechanisms

The two recombination terms in equation (1) correspond to recombination in the quasi-neutral regions of the device (scaling as *1/kT* or *n=1*) and depletion region of the device (scaling as *1/(2kT)* or *n=2*). In relatively wide, direct-bandgap III-V semiconductors it is reasonable to assume that the $n = 1$ recombination corresponds to radiative recombination and $n = 2$ corresponds to non-radiative Shockley-Read-Hall (SRH) recombination. The radiative recombination is calculated from the generalized Planck equation following an approach detailed in [18, 19] that considers the absorptivity of the sub-cell. The non-radiative recombination for the standard GaInP/GaAs/Ge sub-cells is estimated by considering the material quality, parameterized as radiative efficiency, with state-of-the-art material quality corresponding to 30% radiative efficiency at reference conditions (as described in [20]) assumed. However, as the development of the GaAsBi sub-cell is of interest here, the non-radiative recombination for this sub-cell is given in a different form and linked explicitly to the sub-cell configuration and material parameters. This is dependent on SRH minority carrier lifetime and depletion with and given by equation 2.

$$I_{02} = \frac{Wq}{\tau} n_i^2 \tag{2}$$

Equation 2 is the value of the SRH recombination in equation (1), where W is depletion width, q is the charge on an electron, n_i is the intrinsic carrier concentration and τ is the SRH lifetime. The sub-cell voltage is therefore dependent on junction depletion width and minority carrier lifetime.

1.3. Device architecture

There are two principal ways of configuring the junction for a multi-junction solar cell. Due to various reasons such as the formation of a Ge diffused junction using P, and the relative difficulty of achieving high *p*-doping in GaInP, multi-junction cells have the polarity *np* i.e. *p*-type base layers with *n*-type emitter layers on top. The doped *np* junction is one way of configuring the sub-cell. The doping of each layer is increased, increasing the obtainable voltage but decreasing the width of the depletion region. In a solar cell with a diffusion length longer than the absorption depth of the incident light, a short depletion width is desirable since SRH recombination scales with depletion width. However, if the diffusion length is short with respect to the optical absorption depth, field assisted drift transport will be necessary to transport photo-generated carriers. This leads to a compromise between carrier collection and recombination, corresponding ultimately to a trade-off between current and voltage. Here, typical doping values of $1x10^{18}$ cm^{-3} and $1x10^{17}$ cm^{-3} are assumed for the two layers. The emitter is set to 300 nm of the total

GaAsBi thickness. This approach relies on having minority carrier diffusion lengths comparable with the thickness of the layer in question for a particular doping level, as the depleted region will become narrower with higher doping. If minority carrier diffusion lengths are prohibitively short, the alternative *nip* approach is used. The wide *i*-region promotes efficient drift carrier collection due to the electric field present. This approach has been employed successfully for dilute nitride solar cells, which feature short diffusion lengths [21].

To evaluate the possible options available for GaAsBi, both of these approaches, *np* and *nip* are simulated as part of a four-junction solar cell. The resulting cell efficiency under 1000 suns AM1.5D illumination is linked to specific cell parameters – with carrier lifetime affecting recombination and voltage as in equation (2) and short-circuit current determined by varying minority carrier diffusion length in the case of the *np* cell and varying background doping and diffusion length in the *nip* cell. With the exception of one calculation, a value for carrier mobility of 1371 cm^2/Vs as reported by Kini et al. for electron mobility in $GaAs_{0.975}Bi_{0.025}$ [22] is used to link diffusion length with a carrier lifetime.

3. Results

Using the absorption coefficient given in [12], it is found that a thickness of 1.9 μm of GaAsBi is necessary to produce a current-matched 1.9/1.42/1.05/0.66 eV GaInP/GaAs/GaAsBi/Ge cell, assuming perfect collection of photo-generated carriers, 175 μm Ge sub-cell thickness and the ARC described above.

3.1. np-*configuration*

If significant minority carrier diffusion lengths exist then the *np* configuration is desirable since it provides a higher voltage for a given current than an *nip* configuration due to the narrower depletion region. Figure 2 shows the relationship between minority carrier diffusion length and short-circuit current density as determined from the calculation of the quantum efficiency and integration with the AM1.5D spectrum.

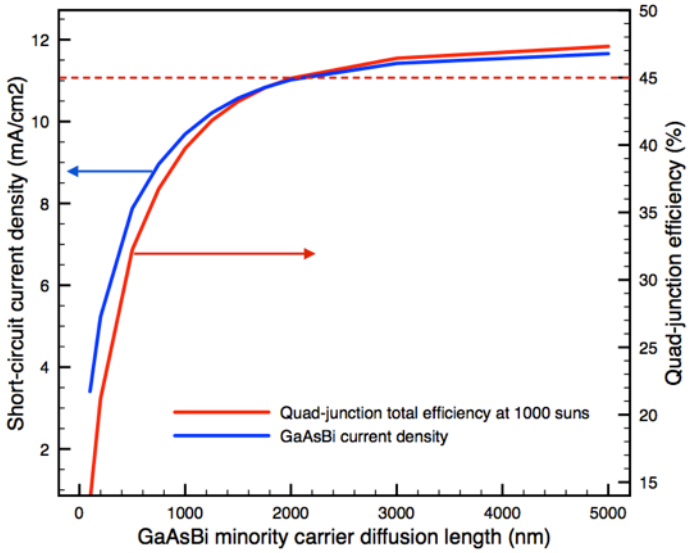

Figure 2. Effect of minority carrier diffusion length (assumed equal for holes and electrons) in an *np* GaAsBi sub-cell on short-circuit current density (at one sun) and overall GaInP/GaAs/GaAsBi/Ge 4J efficiency at 1000 suns. The red dashed line indicates 45% efficiency.

It can be seen that for minority carrier diffusion of the same order of magnitude (2 μm) as the optical thickness of the device, the 4J structure begins to produce >45% efficiency, which is comparable with current records. Figure 3 shows the effect of varying minority carrier lifetime on the sub-cell voltage and overall 4J efficiency. In this calculation the GaAsBi current is fixed for every data point to current-match the other sub-cells. This is done in order to demonstrate that the change in sub-cell voltage corresponding to a change in lifetime of many orders of magnitude has only a minor effect on 4J efficiency under concentrated illumination when compared to the effect caused by loss of current shown in Figure 2. This suggests that in the absence of significant diffusion lengths in the material, a *nip* sub-cell with reduced voltage may still produce a high-efficiency 4J device if it can generate sufficient current. It is interesting to note that when only radiative-recombination is present, the GaAsBi open-circuit voltage is limited to ~0.6V. This is linked to the profile of the absorption coefficient that contains below bandgap tail states [12] and is ultimately goverened by alloy disorder [23]. A semiconductor with an abrupt band-edge, such as InGaAs, would yield a maximum open-circuit voltage of ~0.7V for the same effective optical threshold.

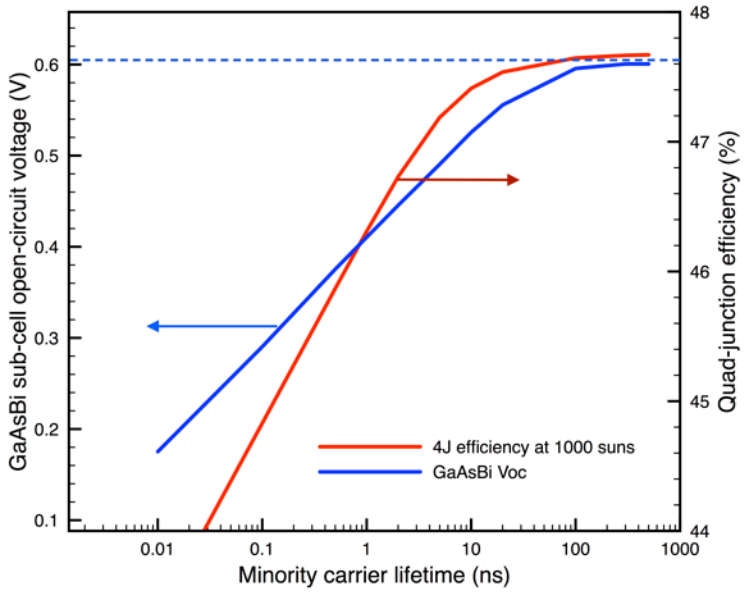

Figure 3. (left) Effect of SRH minority carrier lifetime (assumed equal for holes and electrons) in an *np* GaAsBi sub-cell on open circuit-voltage (at one sun) and overall 4J efficiency at 1000 suns. The blue dashed line indicates the open-circuit voltage at 1 sun when only radiative recombination is present. In this calculation diffusion length has been fixed to provide high current generation in order to demonstrate that the overall quad-junction efficiency is less sensitive to sub-cell current than sub-cell voltage.

3.2 nip-*configuration*

In the nip configuration, the depleted *i*-region is designed to collect all photogenerated carriers across it. However, the *i*-region cannot be made arbitrarily wide since in practice, semiconductor materials have some residual background doping resulting in compensating space charge that limits the width of the depletion region. To investigate this, the 'background' doping in the base region is varied systematically along with potential minority carrier diffusion lengths of the material. Figure 4 shows the effect of independently varying background doping and diffusion length on sub-cell short-circuit current, whereas figure 5 shows the effect on overall 4J efficiency at 1000 suns.

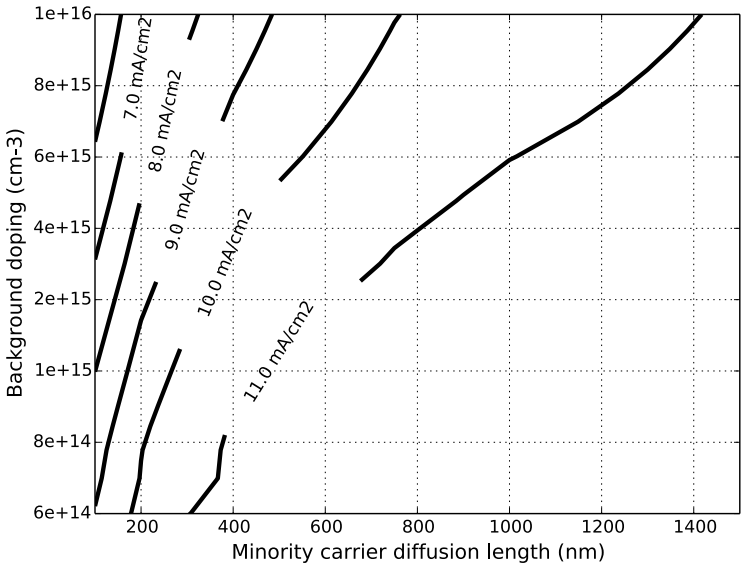

Figure 4. *nip* GaAsBi sub-cell short-circuit current as a function of base doping level and minority carrier diffusion length (equal for holes and electrons) and adjusted for typical reflection and metal grid shading loss. > 11mA/cm^2 should provide high efficiency multi-junction cells.

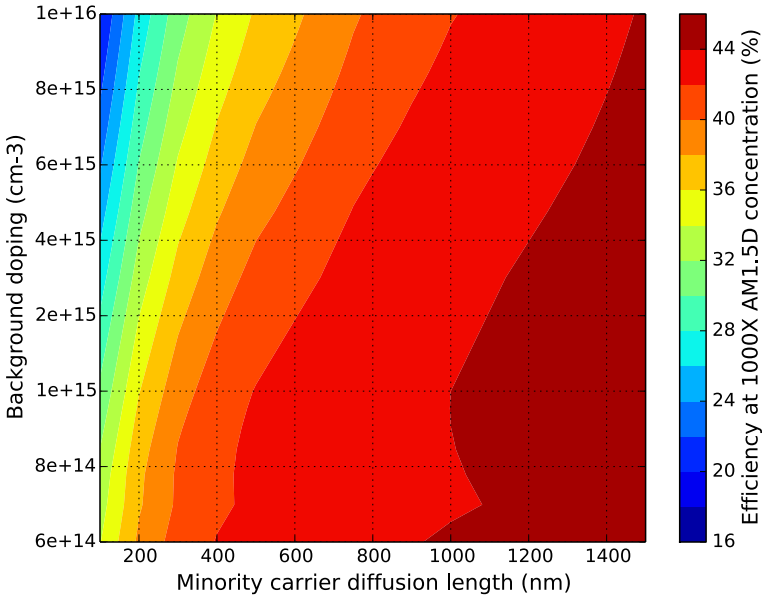

Figure 5. 4J efficiency at 1000 suns as a function of base doping level and minority carrier diffusion length and adjusted for typical extrinsic loss values. The current solar cell efficiency record is 44.7% [1].

4. Discussion

4.1. Simulation results

The results in Figures 2-5 give insight into potential sub-cell designs appropriate for GaAsBi 1 eV sub-cells in a GaInP/GaAs/GaAsBi/Ge quad-junction solar cell. A maximum efficiency of 47.6% is calculated at 1000 suns for a heavily doped, narrow depletion region cell that has material with both long lifetimes and diffusion lengths. This maximum is limited by the values chosen for radiative efficiency, series resistance, anti-reflection coating and grid shading losses and may increase with developments in these areas. If GaAsBi is found to have low diffusion lengths, comparable to dilute nitride materials, then an *nip* structure which sacrifices voltage for greater current gathering may be suitable. Given appropriate control over background doping, high efficiencies >44% may still be reached for this structure. There are several other aspects that may affect cell design – for example, more optimal absorption characteristics through greater understanding of the alloy. The effect of radiative coupling in multi-junction solar cells has also been shown to be of use in cells in which the current is limited by a lower sub-cell [19, 24], especially under concentration, and may allow a given efficiency to be reached with lower GaAsBi sub-cell performance than is calculated here. This effect may also allow for higher band-gap $GaAs_{1-x}Bi_x$ to be used just as effectively as 1.05 eV, necessitating lower Bi content.

4.2 Current status and challenges of $GaAs_{1-x}Bi_x$

Currently the epitaxy of high-quality $GaAs_{1-x}Bi_x$ is complex although we note that room temperature electrically-driven operating bulk [25] and QW [14][26] lasers have now been realized using both MBE and MOCVD growth techniques illustrating the potential and significant progress in the development of these materials. Low growth temperatures have been used to achieve Bi incorporation. The resulting material has been shown to contain a lower defect concentration than low temperature GaAs owing to the surfactant properties of Bi [27]. Bi clusters [28] and surface droplets [29] have been observed, and mechanisms of their formation and control proposed. Growth temperature, growth rate and post-growth annealing interact in complex ways, changing structural and optical quality [30][31][32]. Alloy disorder and carrier localization has also been shown to influence material properties [33]. Full understanding of these factors is likely to be required to produce GaAsBi alloys of sufficient quality to produce a high-efficiency quad-junction solar cell. Furthermore, due to the requirement for 1.9 μm thick GaAsBi with a lattice mismatch of 0.7%, it may be desirable to introduce an element such as N to provide greater lattice matching [6]. There are relatively few reports available on GaAsBi concerning the electrical parameters used in the calculations in this paper. With Bi mainly affecting the valence band, the hole mobility has been shown to reduce much more strongly than the electron mobility with increasing Bi incorporation [34]. In solar cell devices the majority of carriers will be generated in a *p*-type base layer with electrons as the minority carriers. The 1371 cm^2/Vs electron mobility as reported by Kini et al. in [22], if combined with a lifetime of 200 ps [35], would give electron diffusion length of 840 nm. Richards et al. report a background doping density of around $1x10^{16}$ cm^{-3} [36]. From Figure 2 and Figure 5 it can be seen that these parameters may lead to a 4J

efficiency of < 40% if using an *np* GaAsBi sub-cell and > 40% if using an *nip* sub-cell. This shows the importance of knowing the likely achievable parameters when designing sub-cells and reinforces our suggestion that *nip* configuration will be more suitable for GaAsBi sub-cells.

5. Conclusion

GaAsBi has been found to be a promising candidate material for 1 eV sub-cells in multi-junction solar cells. An *np* sub-cell design, while more optimal due to its higher obtainable voltage, will be constrained by the achievable minority carrier diffusion in the material. An *nip* design is less reliant on minority carrier properties but more reliant on control of background doping, and may still provide high efficiencies > 44% as part of a quad-junction GaInP/GaAs/GaAsBi/Ge structure. Other possible architectures, such as a GaInP/GaAs/GaAsBi triple-junction cell or the use of related dilute bismide alloys, may also be of interest.

6. Acknowledgments

T Thomas would like to acknowledge conference attendance funding provided by Climate-KIC as well as EPSRC CASE sponsorship from IQE plc. SJS gratefully acknowledges funding from EPSRC (UK) project EP/H005587/1.

7. References

. [1] Dimroth F et al. 2014 *Prog. in Photovolt.* **22 (3)** 277

. [2] Chiu P et al., 2014 *Proc. IEEE 40th PVSC*

. [3] France R et al., 2014 *Proc. IEEE 40th PVSC*

. [4] Miller N et al., 2014 *Proc. IEEE 40th PVSC*

. [5] Wiemer M, Sabnis V and Yuen H, 2011 *Proc. Of SPIE* **8108** 810804-1

. [6] Sweeney S J and Jin S R, 2013 *J. Appl. Phys.* **113** 043110

. [7] Sweeney S J and Hild K and Jin S R, 2013 *Proc. IEEE 39th PVSC* 2474-2478

. [8] Usman M et al., 2011 *Phys. Rev. B* **84**, 245202

. [9] Geisz J F et al., 2008 *Appl. Phys. Lett.* **93** 123505

. [10] Oe K and Okamoto H, 2000 *Jpn. J. Appl. Phys.* **37** 1283

. [11] Lewis R B and Masnadi-Shirazi M and Tiedje T, 2012 *Appl. Phys. Lett.* **101** 082112

. [12] Hunter C et al., 2012 *IEEE Photonics Technology Letters* **24 (23)** 2191

. [13] Hossain N et al, 2012 *Appl. Phys. Lett.* **100** 051105

. [14] Marko I P et al., 2014 *J. Phys. D: Appl. Phys.* **47** 345103

. [15] Adachi S, 1989 *J. Appl. Phys.,* **66** 6030

. [16] Masnadi-Shirazi M et al., 2014 *J. Appl. Phys.* **116** 223506

. [17] Führer M and Farrell D and Ekins-Daukes N, 2013 *AIP Conference Proceedings* **1556** 34

. [18] Nelson J et al., 1997 *J. Appl. Phys.* **82** 6240

. [19] Thomas T et al., 2014 *Proc. IEEE 40th PVSC*

. [20] Chan N L A et al., 2012 *IEEE J. of Photovolt.* **2 (2)** 202

. [21] Jackrel D B et al., 2007 *J. Appl. Phys.* **101** 114916

. [22] Kini R N et al., 2009 *J. Appl. Phys.* **106 (4)** 043705

. [23] Usman M et al., 2013 *Phys. Rev. B* **87** 115104

. [24] Derkacs D, Bilir T and Sabnis V, 2013 *IEEE J. of Photovolt.* **3 (1)** 520

. [25] Fuyuki T et al., 2014 *Appl. Phys. Express* **7** 082101

. [26] Ludewig P et al., 2013 *Appl. Phys. Lett.* **102** 242115

. [27] Mooney P M et al., 2013 *J. Appl. Phys.* **113** 133708

. [28] Wu M et al., 2014 *Nanotechnology* **25** 205605

. [29] Vardar G et al., 2013 *Appl. Phys. Lett.* **102** 042106

. [30] Moussa I et al., 2008 *Semicond. Sci. Technol.* **23** 125034

. [31] Li J et al., 2014 *J. Appl. Phys.* **116** 043524

. [32] Puustinen J et al., 2013 *J. Appl. Phys.* **114** 243504

. [33] Imhof S et al., 2010 *Appl. Phys. Lett.* **96** 13115

. [34] Kado K et al., 2012 *Jpn. J. Appl. Phys.* **51** 040204

. [35] Mazzucato S et al., 2013 *Semicond. Sci. Technol.* **28** 022001

. [36] Richards R et al., 2013 *Proc. IEEE 39th PVSC* 0303-0305